

INTERACTION OF THE DIHYDROPYRIDINE/PYRIDINIUM REDOX PAIR FIXED INTO A V-SHAPED CONFORMATION

Yasukazu Hirao,^{1*} Mitsuru Teraoka,¹ and Takashi Kubo^{1*}

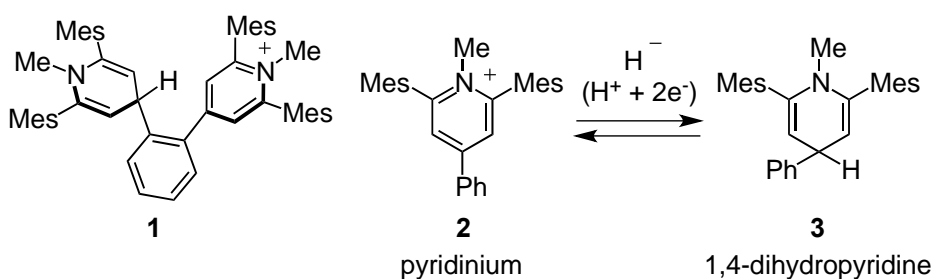
¹ Department of Chemistry, Graduate School of Science, Osaka University, 1-1 Machikaneyama, Toyonaka, Osaka 560-0043, Japan.

e-mail: y-hirao@chem.sci.osaka-u.ac.jp, kubo@chem.sci.osaka-u.ac.jp

Abstract – A new V-shaped molecule incorporating a dihydropyridine and a pyridinium moiety was synthesized and evaluated for its effect on the interaction between the hydride donor-acceptor pair. Spectroscopic, electrochemical, and computational studies have revealed the presence of the charge transfer interaction as a consequence of the electron donor-acceptor association.

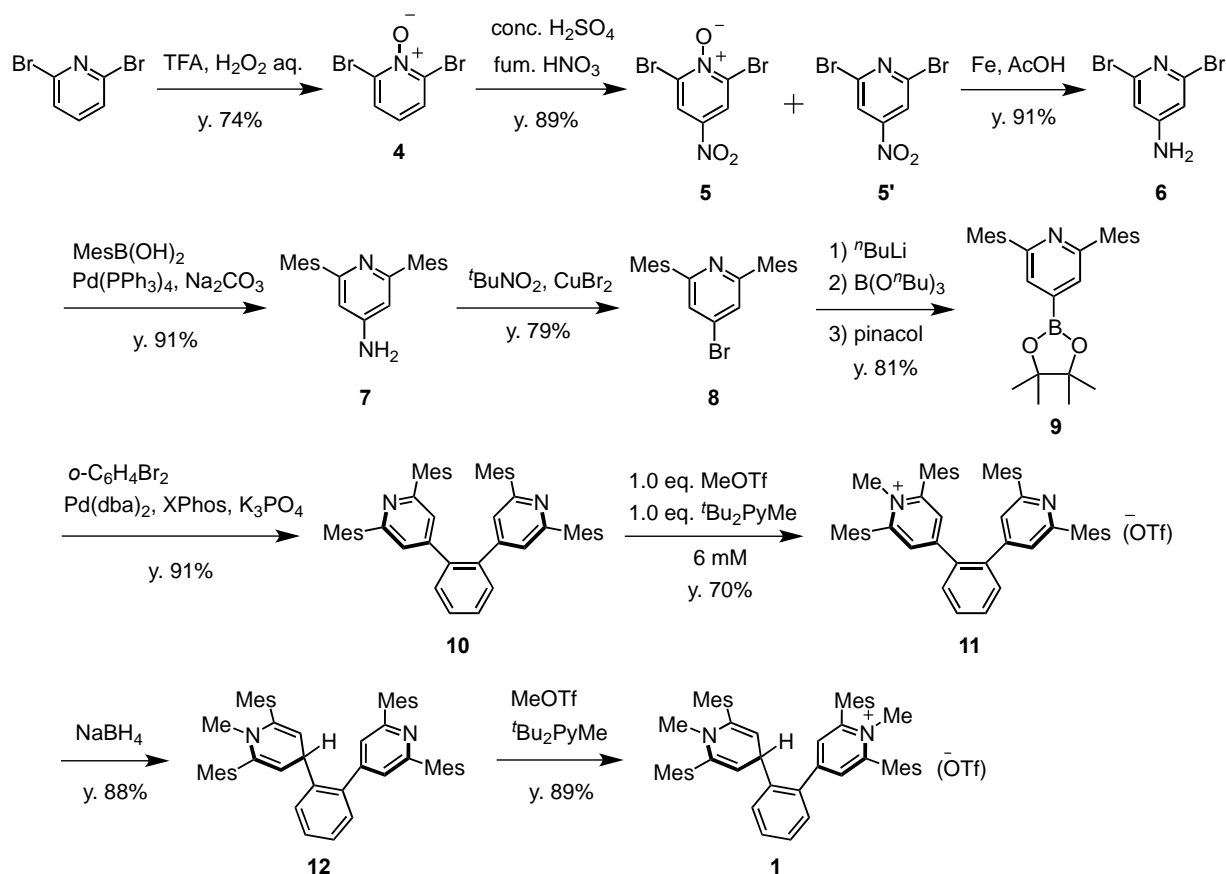
Structural motifs involved in a strongly interacting conjugate donor-acceptor pair in a transfer reaction provide a system similar to the reaction intermediate or transition state, generally leading to a functional electronic structure. For example, in the protonated form of the proton sponge, the 1,8-naphthalene structure promotes proton sharing between the conjugate proton donor-acceptor (acid-base) pair, and thus strongly captures a proton.¹ In another example, π - π stacking between a conjugate electron donor-acceptor pair promotes electron delocalization within a pair, and its function is essential for molecular conductive materials.² Previously, our group also reported the coplanar hydrogen-bonded complex between anthranol and anthroxyl, which is very similar to the transition state structure of the hydrogen atom transfer reaction predicted from theoretical calculations.³ Indeed, the isolated strong hydrogen-bonding allows a hydrogen atom self-exchange confirmed by X-ray analysis. Compared to these proton, electron, and hydrogen atom transfers, to our knowledge, few studies have attempted to isolate the state created by a hydride donor-acceptor pair.^{4,5} Hydride transfer reactions are known to contribute to a critical step in many enzyme systems. Therefore, the reactions between various substrates, such as the transfer from the 4-position of the nicotinamide adenine dinucleotide (NADH/NAD⁺), has been intensively studied to apply them to reduction reactions in vitro.⁶⁻⁹ However, most of studies have analyzed reactions kinetically,¹⁰ and studies focusing on the structural and electronic aspects are mostly limited to theoretical calculations.¹¹

Here we designed and synthesized the V-shaped molecule **1** having a dihydropyridine and its oxidized form pyridinium connected by an *o*-phenylene linker. These units in **1** can be regarded as a conjugate hydride donor-acceptor pair, which are the core structure of the NADH/NAD⁺ coenzyme couple. Exploring the conformational conditions between the hydrogen atom at the 4-position of dihydropyridine and the reaction substrate in the hydrogenation reaction is an important issue in developing further efficient hydride transfer. Thus, the proton at the 4-position of the dihydropyridine moiety involved in the dihydropyridine/pyridinium interactions was studied in detail by spectroscopy and voltammetry methods.



The synthesis of the target compound **1** was carried out according to the Scheme 1.¹² At first, to activate an electrophilic substitution reaction at the 4-position of 2,6-dibromopyridine, *N*-oxidation was conducted with trifluoroacetic acid and hydrogen peroxide. The nitration and subsequent reduction of the nitro group by iron powder afforded the 4-aminopyridine derivative **6**. The substitution of the mesityl groups at the 2,6-positions of the pyridine ring was achieved by the Suzuki-Miyaura coupling reaction with mesitylboronic acid. These two mesityl groups kinetically protect the C2 and C6 carbons of the pyridine ring and expected to contribute to the site-selective hydride reduction at the 4-position. The bromide **8** was obtained by the Sandmeyer reaction of the amine **7**, and then converted to a boronic ester **9** through lithiation and borylation steps. The resulting boronic ester **9** was subjected to the second Suzuki-Miyaura coupling reaction with *o*-dibromobenzene in the presence of a catalytic amount of Pd(dba)₂ and Xphos ligand, affording the symmetrical *o*-disubstituted benzene derivative **10**. To make an unsymmetric compound, only one of the two pyridine rings in **10** had to be *N*-methylated. Therefore, the reaction was performed under dilute conditions (6 mM) using 1.0 equiv. of methyl trifluoromethanesulfonate and 2,6-di-*tert*-butyl-4-methylpyridine (DTBMP) as an acid scavenger base. In the reduction reaction with sodium borohydride, only the *N*-methylated pyridine ring was reacted, and its 4-position was selectively hydrogenated owing to the sterically bulky mesityl group substituted at the 2,6-positions. In fact, phenyl-substituted pyridinium derivatives underwent hydrogenation also at the 2- or 6-position. That is, the steric protection does not work sufficiently with the phenyl group, so the hydrogenation may not proceed site-selectively or stably. The final step of the synthesis is methylation of the other remaining pyridine ring, which proceeded well with methyl trifluoromethanesulfonate and DTBMP. In addition to the target compound **1**, the pyridinium and dihydropyridine moieties contained therein were split into two

molecules **2** and **3**, respectively, which were synthesized according to Scheme S1 to utilize as reference compounds. Here again, the site-selective hydrogenation with sodium borohydride proceeded in good yield to provide the 1,4-dihydropyridine **3**.



Scheme 1. Synthetic route to the V-shaped pyridinium-dihydropyridine system **1**

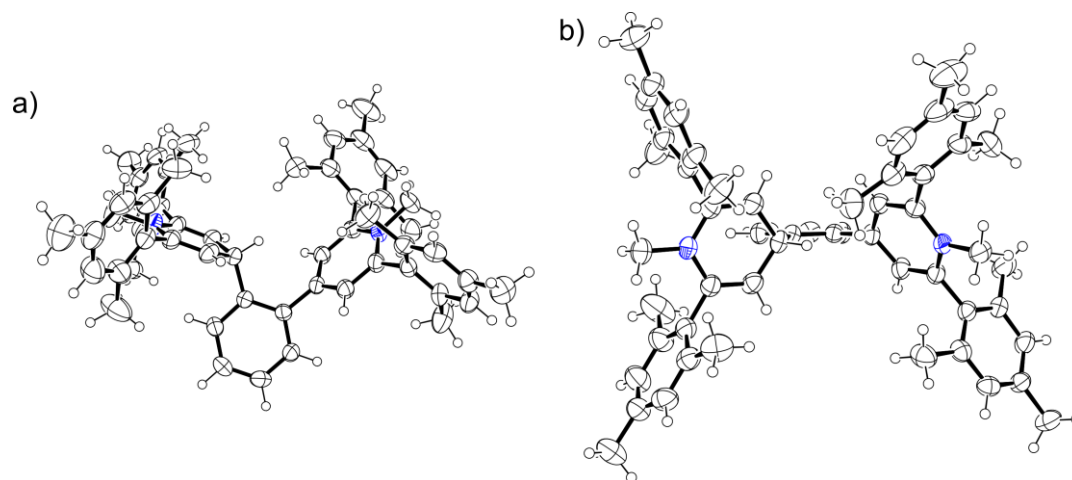
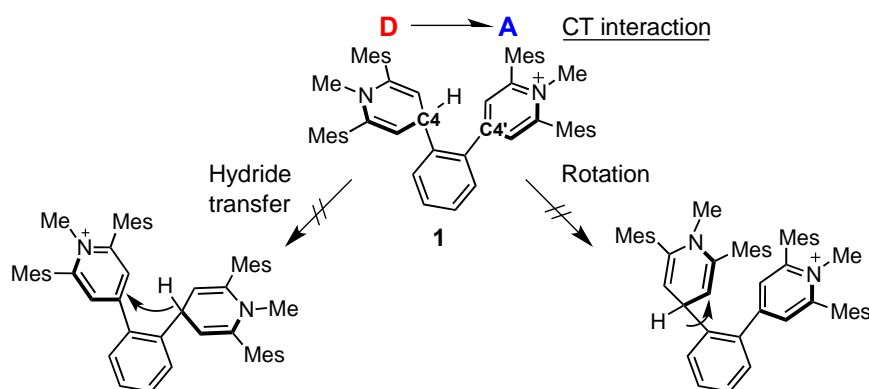


Figure 1. a) Side and b) top views of the ORTEP drawing of **1**. Trifluoromethanesulfonate anion as the counter anion is omitted for clarity.

Vapor diffusion of pentane into the acetone solution of **1** gave orange prism crystals suitable for X-ray crystallographic analysis.¹³ The solved molecular structure of **1** shown in Figure 1 indicates the pyridinium and dihydropyridine rings are arranged facing each other, and the hydrogen atom at the 4-position of dihydropyridine faces inward. In this molecular conformation, the hydrogen atom of interest places within the valley of the V-shape. The molecular conformation in which the hydrogen atoms face outwards may have not been allowed due to the steric repulsion between the bulky mesityl groups (Scheme 2).



Scheme 2. Chemical and physical properties of **1**

The structure of **1** also adopts the same conformation in solution. The NOESY experiment using the acetone-*d*₆ solution sample showed a clear interaction between the proton at the 4-position of the dihydropyridine ring and the protons at the 3- or 5-position of the pyridinium rings, indicating that the C4–H bond is directed toward the inside of the valley (Figures S1 and S2). In addition, no significant temperature dependence was observed in the position and shape of the NMR peaks (acetone-*d*₆: –90 ~ 25 °C and acetonitrile-*d*₃: 30 ~ 70 °C), indicating the absence of the dynamic rotation of the two pyridine rings (Figures S3 and S4). Note that the pyridinium and dihydropyridine moieties are clearly distinguished on the NMR time scale. In addition, the chemical shift of the 4-position methine proton in the dihydropyridine moiety of **1** was not significantly different from that of the precursor **12** and the monomeric compound **3** as reference compounds without interaction (**1**: 4.75 ppm, **3**: 4.55 ppm, and **12**: 4.81 ppm in chloroform-*d*). In the 1,8-naphthalene-linked acridinium-acridan system reported by Suzuki *et al.*, the 1,5-hydride shift, that is the hydride transfer between the acridinium and acridan units, makes it impossible to distinguish both units at room temperature.⁵ They also found a localization of this hydrogen atom on one site at a low temperature of –90 °C. In contrast, even at a high temperature of 70 °C, our pyridinium-dihydropyridine system did not show any coalescence of NMR signals (Figure S4), suggesting that the hydrogen atom of interest is totally localized on one site.

Despite the lack of hydride transfer in **1**, an intramolecular charge-transfer (CT) interaction was observed in electrochemical measurements. Cyclic voltammetry of **1** revealed one irreversible oxidation wave at $E_1 = 0.32$ V (vs. Fc/Fc⁺) and one reversible redox wave at $E_2 = -1.66$ V (vs. Fc/Fc⁺) which are corresponding to the one-electron oxidation process of the dihydropyridine moiety and the one-electron redox process of the pyridinium moiety, respectively (Figure S5). As listed in Table S1, the oxidation potential E_1 of **1** is higher than the corresponding process of the reference dihydropyridine **3** (E_1 vs Fc/Fc⁺ = 0.17 V). Similarly, its redox potential E_2 is slightly lower than that of the reference pyridinium **2** (E_2 vs Fc/Fc⁺ = -1.57 V). These differences originates from the through-space electronic interaction between the electron doping dihydropyridine moiety and the electron accepting pyridinium moiety. The partial electron donating from the dihydropyridine moiety may shift its oxidation potential toward more positive values. In contrast, the through-bond interaction through the *o*-phenylene linker is presumed to be inhibited by greater twisting of the molecular backbone as a result of the steric repulsion from the bulky mesityl groups.

The CT interaction within the V-shaped structure is also revealed by optical spectroscopy. Figure 2 shows the UV-Vis absorption spectra for **1** together with the reference compounds **2** and **3**. Note that the absorption spectrum of **1** is characterized by a weak and broad absorption band around 500 nm, which is not observed in the spectra for the reference single component compounds and their mixtures. This structureless broad band can be attributed to the intramolecular charge transfer (ICT) transition from the dihydropyridine moiety to the pyridinium moiety.¹⁴ Similar to the discussion of the results of the electrochemical measurements, the ICT band probably stems from the presence of the through-space interaction.

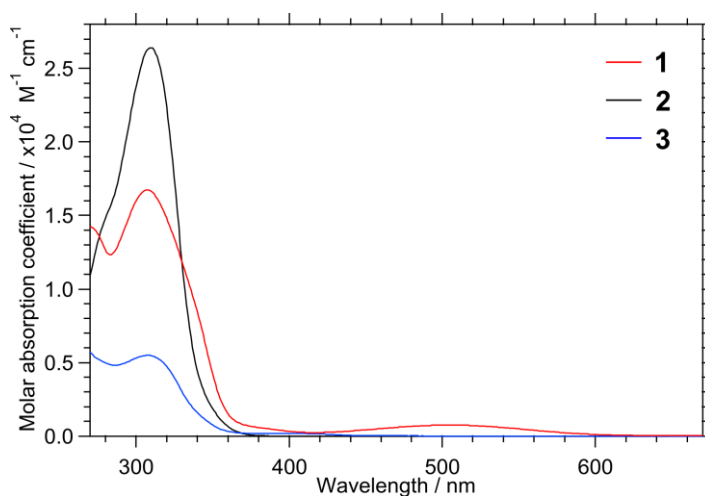


Figure 2. UV-Vis absorption spectra of **1**, **2**, and **3** in dichloromethane

The above specific features characteristic of the V-shaped donor-acceptor system **1** are associated with the electronic interaction between pyridinium and dihydropyridine, but not related to the ability to donate or accept a hydrogen atom (proton or hydride). Moreover, the present system should not be discussed within the scope of sigmatropic rearrangement reactions. As shown in the X-ray structure, because the building blocks in **1** are connected orthogonally, the π orbital of the *o*-phenylene linker cannot mediate the conjugation between the π orbital of the pyridinium moiety and the C4–H σ orbital of the dihydropyridine moiety. Therefore, activation of the reaction between the units at the both ends requires a direct interaction of their molecular orbitals (MOs) through space. Figure 3a depicts the relative orientation and distance between the pyridinium and dihydropyridine moieties in **1**, and the selected distances and angles determined distribution of the frontier orbitals based on the CAM-B3LYP-D3/6-31G** optimized geometry exhibits the HOMO localized at the dihydropyridine moiety and the LUMO localized at the pyridinium moiety (Figure 3b). It is noteworthy that the interaction between the C4–H σ orbital involved in HOMO and the π^* orbital in LUMO is determined to be weak which is due to the deviation of the direction of the involving MOs. This small orbital overlap is a plausible reason why the hydride transfer reaction did not take place. Furthermore, the steric hindrance of the mesityl groups substituted at the 2,6-positions probably prevents the structural change to a face-to-face structure for activating the hydride transfer reaction, which the quantum chemical calculations predicted to be a transition state structure.¹¹

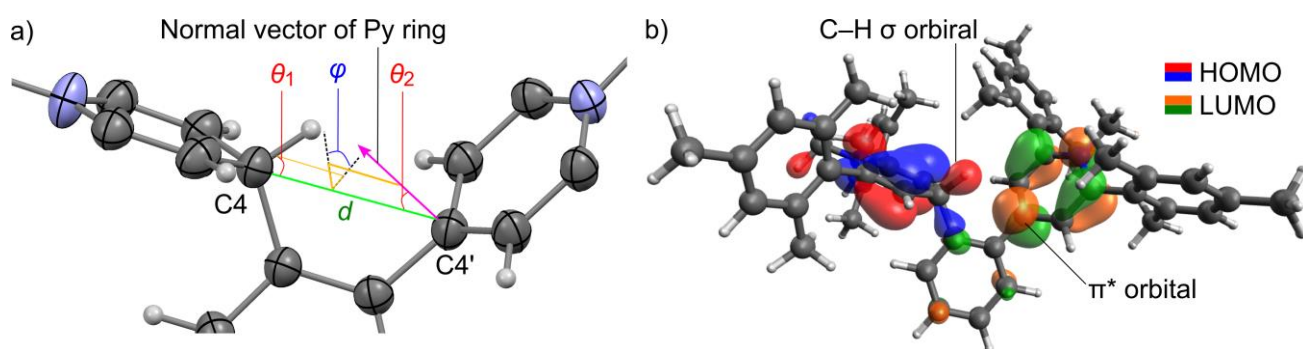


Figure 3. a) Geometrical conformation around the valley of the V-shaped molecule **1** including the definition of the orientation angles. d is the atom-atom distance between the C4 and C4' atoms. θ_1 is the angle between the distance vector and the C4–H bond. θ_2 is the angle between the distance vector and the normal vector of the pyridinium ring. φ is the torsional angle between the C–H bond and the normal vector. The mesityl groups are omitted for clarity. b) DFT optimized geometry and the distribution of the frontier orbitals (isovalue = 0.05 a.u.).

Table 1. Experimentally determined and calculated distances (Å) and angles (°) for the pyridinium-dihydropyridine pair of **1** arranged in a V-shaped orientation

	d	θ_1	θ_2	φ
Exp.	3.018	52.10	37.26	23.86
Calcd.	3.033	53.48	49.27	29.31

Based on the hydride transfer reaction between dihydropyridine and pyridinium, the hydride donor and acceptor units were fixed into a V-shaped orientation by using the *o*-phenylene linker and the bulky substituents. In this conformation, the hydrogen atom at the 4-position of dihydropyridine having the potential to become a hydride source can be located in the valley and is closer to the acceptor pyridinium. Reactions between the units, such as hydride transfer, were not activated, but an intramolecular electron donor-acceptor interaction was observed. This study recognized that the interaction between the hydride donor and acceptor may be dependent on their arrangement, thereby leading to different outcomes such as CT interactions and hydride transfer.

ACKNOWLEDGEMENTS

This work was supported by a Grant-in-Aid for Scientific Research on Innovative Areas “Stimuli-responsive Chemical Species for the Creation of Functional Molecules (No. 2408)” (JSPS KAKENHI Grant Number JP15H00942) from the Ministry of Education, Culture, Sports, Science and Technology, Japan.

SUPPORTING INFORMATION

Supplementary (synthesis, ¹H NMR, etc.) data associated with this article can be found in the online version at URL:

<https://www.heterocycles.jp/https://www.heterocycles.jp/newlibrary/downloads/PDFsi/26517/98/10>.

REFERENCES AND NOTES

1. R. W. Alder, P. S. Bowman, W. R. S. Steel, and D. R. Winterman, *Chem. Commun.*, 1968, 723. “Proton Sponge” is a trademark of Aldrich Chemical Co.
2. J. Ferraris, D. O. Cowan, V. Walatka, Jr., and J. H. Perlstein, *J. Am. Chem. Soc.*, 1973, **95**, 948.
3. Y. Hirao, T. Saito, H. Kurata, and T. Kubo, *Angew. Chem. Int. Ed.*, 2015, **54**, 2402.
4. H. E. Katz, *J. Am. Chem. Soc.*, 1985, **107**, 1420.
5. H. Kawai, T. Takeda, K. Fujiwara, and T. Suzuki, *J. Am. Chem. Soc.*, 2005, **127**, 12172; T. Suzuki, Y. Yoshimoto, T. Takeda, H. Kawai, and K. Fujiwara, *Chem. Eur. J.*, 2009, **15**, 2210.

6. M. M. Hurley and S. Hammes-Schiffer, *J. Phys. Chem. A*, 1997, **101**, 3977; B. Schiøtt, Y.-J. Zheng, and T. C. Bruice, *J. Am. Chem. Soc.*, 1998, **120**, 7192; S. H. Mashraqui and M. A. Karnik, *Chem. Lett.*, 2003, **32**, 1064; Y. Lu, Y. Zhao, K. L. Handoo, and V. D. Parker, *Org. Biomol. Chem.*, 2003, **1**, 173; X.-Q. Zhu, H.-R. Li, Q. Li, T. Ai, J.-Y. Lu, Y. Yang, and J.-P. Cheng, *Chem. Eur. J.*, 2003, **9**, 871; X.-Q. Zhu, L. Cao, Y. Liu, Y. Yang, J.-Y. Lu, J.-S. Wang, and J.-P. Cheng, *Chem. Eur. J.*, 2003, **9**, 3937.
7. J. L. Kurz, R. Hutton, and F. H. Westheimer, *J. Am. Chem. Soc.*, 1961, **83**, 584; F. M. Martens, J. W. Verhoeven, C. A. G. O. Varma, and P. Bergwerf, *J. Photochem.*, 1983, **22**, 99; M. B. Taraban, A. I. Kruppa, N. E. Polyakov, T. V. Leshina, V. Lūsis, D. Muceniece, and G. Duburs, *J. Photochem. Photobiol. A: Chem.*, 1993, **73**, 151; A. I. Kruppa, M. B. Taraban, N. E. Polyakov, T. V. Leshina, V. Lūsis, D. Muceniece, and G. Duburs, *J. Photochem. Photobiol. A: Chem.*, 1993, **73**, 159; N. E. Polyakov, M. B. Taraban, A. I. Kruppa, N. I. Avdievich, V. V. Mokrushin, P. V. Schastnev, T. V. Leshina, V. Lūsis, D. Muceniece, and G. Duburs, *J. Photochem. Photobiol. A: Chem.*, 1993, **74**, 75.
8. U. Eisner and J. Kuthan, *Chem. Rev.*, 1972, **72**, 1; D. M. Stout and A. I. Meyers, *Chem. Rev.*, 1982, **82**, 223; R. Lavilla, *J. Chem. Soc., Perkin Trans. 1*, 2002, 1141.
9. G. D. Hartman, B. T. Phillips, W. Halczenko, J. P. Springer, and J. Hirshfield, *J. Org. Chem.*, 1987, **52**, 1136; Y. Inoue, S. Imaizumi, H. Itoh, T. Shinya, H. Hashimoto, and S. Miyano, *Bull. Chem. Soc. Jpn.*, 1988, **61**, 3020; L. D. Guanaes, D. R. B. Ducatti, M. E. R. Duarte, S. M. W. Barreira, M. D. Nosedá, and A. G. Gonçalves, *Tetrahedron Lett.*, 2015, **56**, 2001.
10. E.-U. Würthwein, G. Lang, L. H. Schappele, and H. Mayr, *J. Am. Chem. Soc.*, 2002, **124**, 4084; X.-Q. Zhu, Y. Liu, B.-J. Zhao, and J.-P. Cheng, *J. Org. Chem.*, 2001, **66**, 370; X.-Q. Zhu, F.-H. Deng, J.-D. Yang, X.-T. Li, Q. Chen, N.-P. Lei, F.-K. Meng, X.-P. Zhao, S.-H. Han, E.-J. Hao, and Y.-Y. Mu, *Org. Biomol. Chem.*, 2013, **11**, 6071.
11. Y.-D. Wu, D. K. W. Lai, and K. N. Houk, *J. Am. Chem. Soc.*, 1995, **117**, 4100; J. Andrés, V. Moliner, V. S. Safont, L. R. Domingo, and M. T. Picher, *J. Org. Chem.*, 1996, **61**, 7777; S. Hammes-Schiffer, *ChemPhysChem*, 2002, **3**, 33.
12. The isolated product **1** was contaminated with 3-4 mol% of the dication **14** (Scheme S2). The NMR spectrum of the independently synthesized **14** provided an accurate identification of this contaminant (Figure S6). Two singlet peaks “x” and “y” corresponding to the dication **14** were slightly observed in the NMR spectrum of **1** (Figure S1). The molar ratio was estimated on the basis of the peak height ratio of the “x” and “a” peaks. The NMR peaks from the *o*-phenylene linker for **14** were buried in the baseline because they are broad signals with double-doublet splitting pattern. The peaks from the mesityl substituents overlapped with those of **1**. The contamination is not only due to the difficulty in the purification process. By air-oxidation or photo-oxidation, the dihydropyridine moiety of **1** is

gradually oxidized into pyridinium, and the dicationic species **14** is provided (Scheme S2). The decomposition process of dihydropyridine has already been reported by several groups.¹⁵

13. Crystallographic data for **1**: C₅₄H₅₉N₂·CF₃O₃S, FW = 885.10, orthorhombic, space group *P2₁2₁2₁* (no.19), *a* = 15.2894(4) Å, *b* = 17.1845(4) Å, *c* = 18.5033(4) Å, *V* = 4861.6(2) Å³, *Z* = 4, *D*_{calcd} = 1.209 g·cm⁻³, *T* = 200 K, *R*₁[*I* > 2σ(*I*)] = 0.0606, *wR*₂(all data) = 0.1800, Flack parameter = 0.063(15) for 591 parameters and 9143 independent reflections, GOF = 1.034.
14. The TD-DFT calculation (TD-CAM-B3LYP-D3/6-31G**//CAM-B3LYP-D3/6-31G**) predicted the wavelength of the HOMO-LUMO transition attributable to the ICT as 479.45 nm (*f* = 0.0152), which is in good agreement with the experimental result.
15. S. L. Johnson and P. T. Tuazon, [Biochemistry, 1977, 16, 1175](#); J. Ludvík, J. Volke, and F. Pragst, [J. Electroanal. Chem., 1986, 215, 179](#); C. Selvaraju and P. Ramamurthy, [Chem. Eur. J., 2004, 10, 2253](#); X. Yang, J. Walpita, D. Zhou, H. L. Luk, S. Vyas, R. S. Khnayzer, S. C. Tiwari, K. Diri, C. M. Hadad, F. N. Castellano, A. I. Krylov, and K. D. Glusac, [J. Phys. Chem. B, 2013, 117, 15290](#).